

Title	Optical second harmonic generation analysis of the atomically stepped Au/TiO ₂ (320) interface
Author(s)	Haque, Md Ehasanul; Kobayashi, Daiki; Tomatsu, Yuki; Hien, Khuat Thi Thu; Mizutani, Goro; Rahman, Mohammad Mizanur; Rutt, Harvey N.
Citation	AIP Advances, 7(12): 125011-1-125011-10
Issue Date	2017-12
Type	Journal Article
Text version	publisher
URL	http://hdl.handle.net/10119/15082
Rights	Copyright 2017 Author(s). All article content, except where otherwise noted, is licensed under a Creative Commons Attribution (CC BY) license (http://creativecommons.org/licenses/by/4.0/). The following article appeared in Md Ehasanul Haque, Daiki Kobayashi, Yuki Tomatsu, Khuat Thi Thu Hien, Goro Mizutani, Mohammad Mizanur Rahman, and Harvey N. Rutt, AIP Advances, 7(12), 125011 (2017) and may be found at http://dx.doi.org/10.1063/1.5006847
Description	

Optical second harmonic generation analysis of the atomically stepped Au/TiO₂ (320) interface

Md Ehasanul Haque,¹ Daiki Kobayashi,¹ Yuki Tomatsu,¹ Khuat Thi Thu Hien,¹ Goro Mizutani,^{1,a} Mohammad Mizanur Rahman,² and Harvey N. Rutt³

¹*School of Materials Science, Japan Advanced Institute of Science and Technology (JAIST), 1-1 Asahidai, Nomi, Ishikawa 923-1292, Japan*

²*Department of Physics, University of Dhaka, Dhaka 1000, Bangladesh*

³*School of Electronic and Computer Science, University of Southampton, Southampton SO17 1BJ, UK*

(Received 28 September 2017; accepted 1 December 2017; published online 11 December 2017)

A gold thin film with the thickness of 2nm on the TiO₂(320) substrate has been fabricated in a UHV chamber at the pressure of 2×10^{-7} Torr. We observed the second harmonic response from the Au/TiO₂(320) interface and bare TiO₂(320) as a function of the rotation angle around the surface normal by using of a pulsed Nd³⁺:YAG laser as the excitation light at a photon energy of 1.17 eV and 2.33 eV. An isotropic response was observed from both samples for 1.17 eV photon energy excitation. In contrast, an anisotropic response was observed from both samples for 2.33 eV photon energy excitation. From the Au/TiO₂(320) interface, anisotropic structure of SHG response was observed in the $[\bar{2}30]$ direction for Pin/Pout polarization combination. Nonlinear susceptibility elements were decomposed and two groups of them were assigned as the main contribution from the step and terrace of the vicinal TiO₂ surface. © 2017 Author(s). All article content, except where otherwise noted, is licensed under a Creative Commons Attribution (CC BY) license (<http://creativecommons.org/licenses/by/4.0/>). <https://doi.org/10.1063/1.5006847>

I. INTRODUCTION

The Au/TiO₂ interface is a well-known catalyst for many chemical reactions, especially for the oxidation of CO gas at room temperature.¹⁻³ Gold and titanium dioxide can exhibit catalytic activity when they exist separately. However, the combination of Au and the TiO₂ substrate can work as a tremendous catalyst especially for the oxidation of carbon monoxide.⁴ Haruta *et al.* found that when Au/TiO₂ has long perimeters of the interfaces of the Au and TiO₂ particles, it shows high catalytic activity.⁵ When Tsubota *et al.* studied practical catalyst of mixed Au colloids and TiO₂ powder, it did not show catalytic activity, while it showed high catalytic activity when the tight junction contact was formed between Au colloids and TiO₂ powder by calcination.⁶ This result indicates that the effect of the perimeter of a joining interface exhibit better catalytic activity. However, the role of Au/TiO₂ interface as a catalyst for many chemical reactions and the corresponding electronic phenomena taking place at the active sites are not yet clear.⁷

Indeed, the catalytic activity should depend on the structure such as oxygen vacancies, step structure and crystal imperfections and electronic states of the Au/TiO₂ interface.⁸ So far many researchers studied the electronic states of the Au/TiO₂ interface by using various techniques. Lai *et al.* studied the electronic structure of Au/TiO₂ interface as a function of different Au particle size by STM. They found that the bandgap of the TiO₂ (110) surface is related to the particle size of Au.⁹ Tanaka *et al.* observed the local distribution of interstitial titanium ions in Au/TiO₂ by using an aberration corrected transmission electron microscope. They suggested that interstitial Ti ions are deficient in the peripheral region of Au nanoparticle whereas they existed at the perimeter of the Au

^aCorresponding author: mizutani@jaist.ac.jp.

and TiO₂ particle interface.¹⁰ Yao *et al.* measured the broad absorption peak at the visible region from the particle size-dependent Au/TiO₂ catalyst by using UV-vis reflectance spectra. They concluded that the observed peak was due to the localized surface plasmon resonance of the Au nanoparticles.² A strong absorption peak was observed due to the excitation of Au nanoparticle plasmons from the Au/TiO₂ interface reported by other researchers.^{11–14} We believe that the precise measurement of atomic scale electronic state from Au/TiO₂ interface using specific surface and interface probe such as second harmonic generation (SHG) is desirable. However, the number of studies of the electronic states from the stepped Au/TiO₂ interface by SHG is very limited.

Only a single report was found regarding the observation of the SHG signal from a Au/TiO₂ interface. Quelin *et al.* measured SHG intensity as a function of incident angle and input and output polarization from the thin Au/TiO₂ cermet films. Cermet films are the combination of the ceramic and metallic materials. The Au particles are randomly distributed in the TiO₂ matrix to form a cermet film. They detected enhanced SHG signal due to the local field enhancement by the surface plasmon excitation on gold clusters.¹⁵ In fact, they studied the electromagnetic mode on Au clusters embedded in TiO₂ and were not interested in atomic scale electronic states at the interface between the two materials.¹⁵ For this reason, our aim is to observe the atomic level electronic states of the stepped Au/TiO₂ interface using SHG method.

SHG is forbidden in the bulk of a medium with inversion symmetry within the electric dipole approximation.¹⁶ It has submonolayer sensitivity to the surface and interface of centrosymmetric media because it is only allowed in non-centrosymmetric media.¹⁶ Another attractive feature of SHG is that it is non-invasive and contactless and it can be applied to “in situ” and in “real-time” experiments with a good time resolution.¹⁷ We can deduce information such as electronic structure and molecular orientation from the precise determination of the nonlinear susceptibility tensor.¹⁸ We can extract the electronic level information from the interface of Au/TiO₂.

In fact, many researchers observed the SHG response from the flat and stepped bare TiO₂ surface to understand the electronic states of the surface. Kobayashi *et al.* observed SHG response from TiO₂ (110) as a function of the polarization and azimuthal angle. They determined surface $\chi_{Sijk}^{(2)}$ elements and compared the theoretical patterns with that obtained from the experiment. They concluded that the SHG signal originates from a surface electric dipole.¹⁹ Omote *et al.* studied the SHG spectra as a function of the photon energy from the TiO₂ (110) and (001) surface. In order to study the surface electronic structure, they conducted phenomenological analysis to separate the contribution from various nonlinear susceptibility elements, and the dominant contribution was observed from the surface $\chi_{Sijk}^{(2)}$ elements.²⁰ They also detected a small contribution of the bulk quadrupoles. They performed an *ab initio* calculation by using the FLAPW method within the local density approximation and found that Ti-O-Ti-O- chains including the bridging oxygen atoms on the surface act as the main origin of the SHG signal generation from the TiO₂ (110) surface.²⁰ Takahashi *et al.* detected contribution of steps by comparing the SHG spectra from three kinds of stepped surfaces, TiO₂ (15 15 4), (13 9 0) and (671) with that from a flat (110) surface. They observed large SHG intensity from the step surfaces compared to the flat (110) surface.⁸ They successfully separated the step contribution of surface $\chi_{Sijk}^{(2)}$ elements from stepped surfaces, TiO₂ (15 15 4), (13 9 0) and (671), respectively, because the symmetry was broken at the periodic steps within the surface plane.⁸ In another report,²¹ they observed strong SHG/SFG responses from the stepped TiO₂ (17 18 1) and (15 13 0) surfaces compared to the flat (011) and (110) faces in order to understand the electronic states of terraces and steps. The resonances in the SHG and SFG spectra for each sample suggested that they are due to the valence-conduction interband electronic transitions at the steps. More specifically the local density of states at the step of the vicinal surfaces is distributed right below the valence band maximum (VBM) and right above the conduction band minimum (CBM).²¹

As it is well known, surface defects such as steps and kinks play an important role in generating active sites for catalytic reactions, so it is vital to study the structure and the electronic states of such surface defects in order to understand their catalytic performances. Thus it would be very informative to analyse the SHG response from the interface of TiO₂ atomic stepped surface decorated by Au. In this research, a rutile type TiO₂ (320) single crystal surface with a step height of 0.3 nm was used as a substrate. So far as we know, there has been no previous observation of SHG from the Au/ stepped TiO₂ interface.

In this work, we attempted to detect an optical second harmonic generation signal from steps on the TiO_2 surface decorated by a Au film of 2 nm thickness and tried to separate the terrace and step contributions. On the TiO_2 (320) surface plane there is a structural asymmetry in the $[\bar{2}30]$ direction and this should induce SHG. We measured azimuthal angle and polarization dependent SHG intensity patterns at photon energies 1.17 eV and 2.33 eV for Au/ TiO_2 (320) and TiO_2 (320) samples. We calculated the second order nonlinear optical susceptibility elements from the experimental results and separated the step and terrace contributions from both the samples. This analysis provides an important step for the future SHG spectroscopy of the electronic states of the Au/ TiO_2 (320) interface as a function of the photon energy and the spectrum will be closely related to the catalytic activity of this interface.

II. Experimental

A. Sample preparation

A rutile type TiO_2 (320) single crystal cut from a TiO_2 (110) wafer with 11.3° miscut angle toward the $[1\bar{1}0]$ direction and mirror-polished on one side with thickness of 0.5 mm, was purchased from K & R Creation Co., Ltd. The sample should have periodic 0.3nm atomic steps after annealing appropriately. It was etched in 5% hydrofluoric (HF) acid solution for 10 minutes to remove the impurities on the surface and rinsed with pure water. After etching it was annealed in air at 800°C for 2 hours to remove the bulk oxygen vacancies. Then, the sample was cleaned with ethanol, acetone and pure water in an ultrasonic cleaner. Finally, the sample was placed in a UHV chamber at pressure 2×10^{-7} Torr and Au was deposited with thickness of 2 nm at a deposition rate of about 0.1 nm/sec controlled by using a thickness monitor.

The surface structure of the bare TiO_2 (320) single crystal and deposited 2 nm Au thin film was checked by using AFM. Figure 1(a) shows clearly the regular periodic step on the bare TiO_2 . In Fig. 1(b), an island structure was observed on the Au surface with the maximum length and height of the island about 400 nm and 200 nm, respectively. In order to confirm the distribution of Au, we used SEM with EDX. From these measurement, we found gold nanoparticles which are embedded in a thin continuous gold film covering the entire surface, including the steps. Therefore,

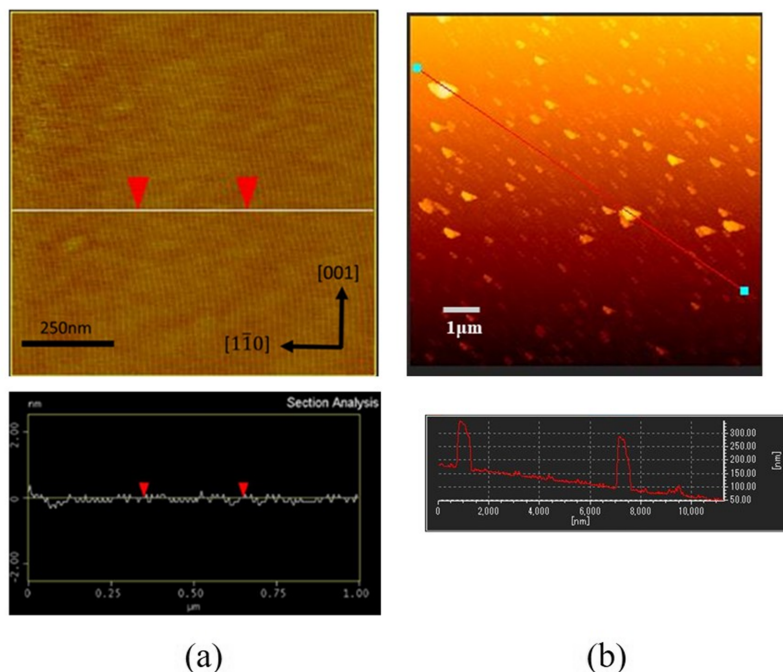


FIG. 1. AFM images and profiles of (a) bare TiO_2 (320) and (b) Au deposited TiO_2 (320).

equation²³

$$P_{NL,i}(2\omega) = \sum_{j,k=y,z} \epsilon_o \chi_{Sijk}^{(2)} : E_j(\omega) E_k(\omega) \quad (1)$$

Here, $P_{NL,i}(2\omega)$ is the second order nonlinear polarization, ϵ_o is the permittivity of the free space, $\chi_{Sijk}^{(2)}$ is the surface nonlinear optical susceptibility, $E_j(\omega)$ and $E_k(\omega)$ are the incident electric field. We can find a guideline in a textbook²⁴ on how to calculate a nonlinear susceptibility of a sheet layer using hyperpolarizabilities of adsorbed molecules or interface steps and on how to calculate an electromagnetic wave amplitude emitted by this sheet. We calculated SHG intensity patterns and the peak intensities from the dielectric structure for the Au/TiO₂ (320) face, when one of the 10 surface nonlinear susceptibility elements $\chi_{Sijk}^{(2)}$ is set equal to a common value and the other elements are all set equal to zero. The result is independent of the thickness and the dielectric function of the second layer because of the advantage of the usage of surface nonlinear susceptibility elements $\chi_{Sijk}^{(2)}$. We then fit the theoretical SHG intensity patterns to those obtained in the experiment. We calculated the linear combinations of the patterns originating from the $\chi_{Sijk}^{(2)}$ elements in the complex plane with each pattern multiplied by the relevant nonlinear susceptibility element and then varied the nonlinear susceptibility elements as adjustable parameters. We fit the patterns by the least square fitting method.

IV. RESULTS AND DISCUSSION

Figures 3 and 4 show the azimuthal angle dependent SHG intensity patterns with four different input and output polarization combinations of Pin/Pout, Pin/Sout, Sin/Pout and Sin/Sout from the Au/TiO₂ (320) interface and the bare TiO₂ (320) surface with the incident photon energy 1.17 eV and 2.33 eV in air. The dots and lines represent the experimental and calculated data, respectively. Figures 3 show that the SHG response from both Au/TiO₂ (320) and bare TiO₂ (320) samples are isotropic when we used excitation photon energy of 1.17 eV. On the other hand, anisotropic behavior is seen from both samples for at 2.33 eV as shown in Figs. 4. In general, when the energy of two photon excitation is larger than the band gap of TiO₂ an electronic resonance will be observed. In Fig. 3 the two photon energy of 2.34 eV of 1064 nm excitation is smaller than the bandgap of TiO₂

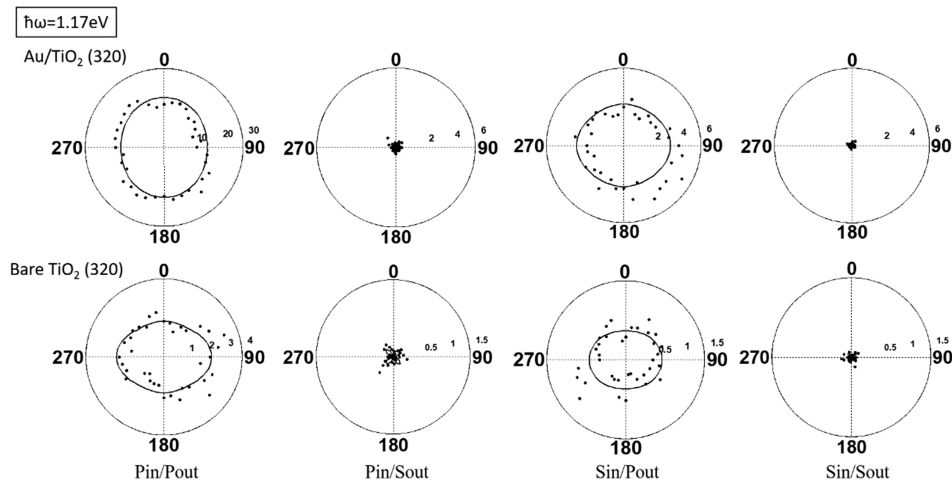


FIG. 3. SHG intensity patterns as a function of the azimuthal angle φ for the four different input and output polarization combinations from the Au/TiO₂ (320) interface and from the bare TiO₂ (320) surface with excitation photon energy $\hbar\omega=1.17\text{eV}$. The SHG intensity is plotted in the radial direction in an arbitrary but common unit. The input and the output polarizations are shown at the bottom, such as Pin/Sout for P-polarized input and S-polarized output. The azimuthal angle φ is defined as the rotation angle around the surface normal of the sample. The zero degree of φ corresponds to the configuration when the plane of incidence includes the $[2\bar{3}0]$ direction. The incidence angle was set at 45° . The dots and lines represent the experimental and calculated data, respectively.

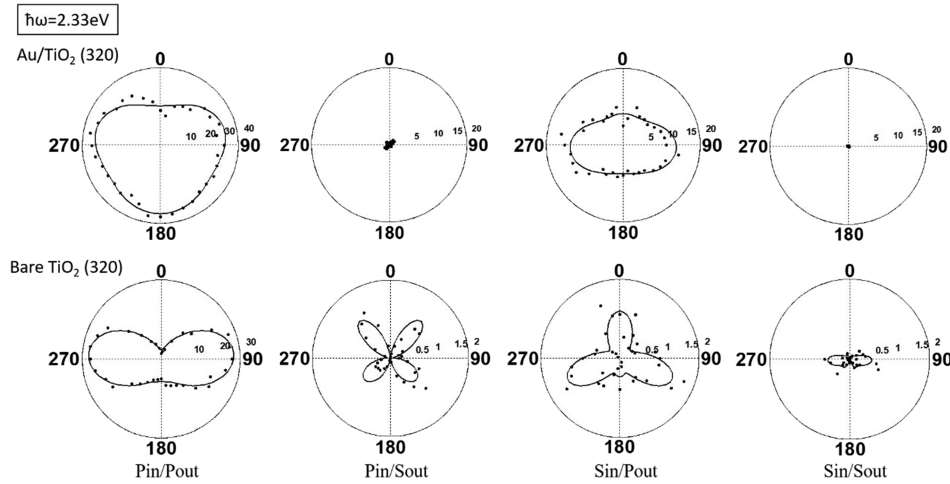


FIG. 4. SHG intensity patterns as a function of the azimuthal angle φ for the four different input and output polarization combinations from the Au/TiO₂ (320) interface and from the bare TiO₂ (320) surface with excitation photon energy $\hbar\omega=2.33\text{eV}$. The SHG intensity is plotted in the radial direction in an arbitrary but common unit. The input and the output polarizations are shown at the bottom, such as Pin/Sout for P-polarized input and S-polarized output. The azimuthal angle φ is defined as the rotation angle around the surface normal of the sample. The zero degree of φ corresponds to the configuration when the plane of incidence includes the $[\bar{2}30]$ direction. The incidence angle was set at 45° . The dots and lines represent the experimental and calculated data, respectively.

(3.05 eV) so that the electronic resonance did not occur. This is the reason for the isotropic SHG response from both Au/TiO₂ (320) and bare TiO₂ (320) samples. In Fig. 4 the two photon energy 4.66 eV of 532 nm excitation is larger than the bandgap of TiO₂ and hence anisotropic responses were observed. From the experimental SHG intensity patterns, we applied a least square fitting algorithm and the results are shown by lines in Figs. 3 and 4. We conducted the phenomenological analysis of the SHG intensity patterns using nonlinear optical susceptibility.²⁵

In the theoretical calculation, nono-zero $\chi_{ijk}^{(2)}$ elements²⁶ are decided by the symmetry of the structures of the Au/TiO₂ (320) and bare TiO₂ (320) samples, namely C_s symmetry. Then we have ten independent nonlinear susceptibility elements, $\chi_{223}^{(2)} = \chi_{232}^{(2)}$, $\chi_{113}^{(2)} = \chi_{131}^{(2)}$, $\chi_{112}^{(2)} = \chi_{121}^{(2)}$, $\chi_{211}^{(2)}$, $\chi_{222}^{(2)}$, $\chi_{233}^{(2)}$, $\chi_{323}^{(2)} = \chi_{332}^{(2)}$, $\chi_{311}^{(2)}$, $\chi_{322}^{(2)}$, and $\chi_{333}^{(2)}$. Here 1, 2, and 3 represent the [001], $[\bar{2}30]$, and [320] directions on the stepped TiO₂ (320) surface, respectively, and their axes are fixed to the sample as shown in Fig. 5. The mirror plane of the surface structure is the 2-3 plane. In the directions 2 and 3 there are broken symmetries caused by the surface steps and the terrace surface, respectively. Hence the nonlinear susceptibility elements $\chi_{121}^{(2)}$, $\chi_{211}^{(2)}$, $\chi_{222}^{(2)}$, $\chi_{233}^{(2)}$, and $\chi_{323}^{(2)}$ with odd number of suffices 2 originate from the step contribution. The other five susceptibilities $\chi_{113}^{(2)}$, $\chi_{223}^{(2)}$, $\chi_{311}^{(2)}$, $\chi_{322}^{(2)}$, and $\chi_{333}^{(2)}$ with odd numbers of suffices 3 originate from the terrace contribution. Here the terrace contribution contains both that from the TiO₂ (110) terrace and that from the Au film surface.

By using the ten evaluated $\chi_{ijk}^{(2)}$ elements we separated the theoretical SHG intensity patterns into those of the terrace and step contributions. However, at the excitation photon energy 1.17 eV, the SHG intensity from the step contribution of the Au/TiO₂ (320) interface are 0.2 and 0.15, in an arbitrary but common unit throughout this paper, for Pin/Pout and Sin/Pout polarization combinations, respectively, and they were smaller than the noise amplitude of approximately 0.5. For this reason, the fitting of the experimental data in Fig. 3 is conducted by considering only the terrace group of $\chi_{ijk}^{(2)}$ elements. Similarly, for the step contribution of the bare TiO₂ (320) surface, the SHG intensity is 0.1 and 0.2, in an arbitrary but common unit for the Pin/Pout and Sin/Pout polarization combinations, respectively. They are much smaller than the terrace contribution and are below the noise level. The simulated SHG intensity patterns for Pin/Sout and Sin/Sout for both the Au/TiO₂ (320) and bare TiO₂ (320) were very weak. Therefore, we consider, their contributions are negligible.

On the other hand, at the excitation photon energy of 2.33eV, the step contribution was clearly larger than the noise. The calculated SHG intensity patterns for both Au/TiO₂ (320) and

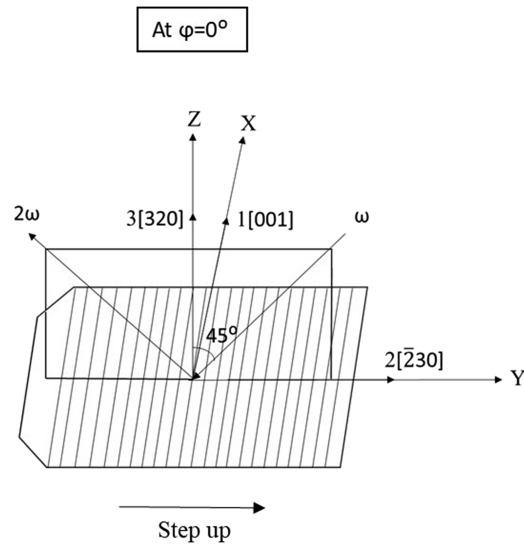


FIG. 5. Schematic diagram of the stepped TiO_2 (320) substrate with the incidence plane. Here the coordinate symbols are (X, Y, Z) =Laboratory Coordinates and $(1, 2, 3)$ =Sample Coordinate. The sample coordinates are indicated by $1[001]$, $2[\bar{2}30]$ and $3[320]$ directions. The azimuthal angle φ is the angle between X and the axis 1. The angle φ equals to zero when X and the axis 1 are on the same direction as illustrated above. The mirror plane of the surface structure is the 2-3 plane. In a more specific way, direction 2 is parallel to surface that lies in the mirror plane of TiO_2 and perpendicular to step edge where the symmetry is broken and direction 3 is perpendicular to the surface of the stepped TiO_2 sample. At $\varphi = 0^\circ$, direction 2 corresponds to the step up direction and it is same direction with laboratory coordinate Y .

bare TiO_2 (320) samples are shown in Fig. 6 for excitation at 2.33 eV separated into the terrace and step contributions. The simulated SHG intensity patterns for Pin/Sout and Sin/Sout for the Au/ TiO_2 (320) were very weak. The terrace contribution for Sin/Sout for the bare TiO_2 (320) was

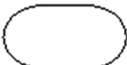

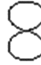
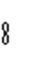
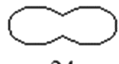

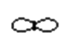




Sample	$\chi_{ijk}^{(2)}$	Pin - Pout	Pin - Sout	Sin - Pout	Sin - Sout
Au/ TiO_2 (320) (532 nm)	Au/ TiO_2 terrace contribution	 33		 12.5	
	Au/ TiO_2 step contribution	 10		 0.2	
Bare TiO_2 (320) (532 nm)	TiO_2 terrace contribution	 24	 0.5	 1	
	TiO_2 step contribution	 0.6	 0.5	 0.6	 0.5

FIG. 6. The calculated SHG intensity patterns for Au/ TiO_2 (320) and bare TiO_2 (320) based from the terrace and step contributions fitted to the experimental results with photon excitation energies of 2.33eV. The SHG intensity is plotted in the radial direction in an arbitrary but common unit.

weak. Their contributions are negligible and the corresponding intensity patterns are not shown in Fig. 6.

From the above simulation results of the step and terrace groups of $\chi_{ijk}^{(2)}$ elements, one can see that the step contribution from the Au/TiO₂ (320) is different from that of the step contribution from the bare TiO₂ (320) sample for the Pin/Pout polarization combination, as we can see it in Fig. 6. Also for the Sin/Sout polarization combination in Fig. 4, the bare surface shows a finite intensity, while the Au/TiO₂ (320) gives a negligible signal for Sin/Sout polarization combination as in Fig. 4. In order to discuss the possible reasons for this difference, we considered the following candidates of the origins of the step contribution to the signal of the Au/TiO₂ (320) interface.

A. Enhancement of the incident electric field by surface defects

Surface defects such as crystal imperfections, island structures, steps and kinks are considered as a candidate origin for the electric field enhancement. The defects on the surface/interface may act as the “hot spot” and the local field can be concentrated and coupling may occur strongly. These couplings were the origin of the enhancement of the incident electric field.²⁷ Namely, C. K. Chen *et al.* observed a large enhancement of SHG signal from the roughened silver surface compared to a smooth surface due to the enhancement of the electric field by the roughness.²⁸ From Fig. 1(b), we found that Au deposited TiO₂ (320) surface contains island structure and these islands might act as “hot spot” and make the SHG intensity stronger. However, this effect should have an isotropic nature with respect to the rotation of the sample around its normal because these islands are randomly distributed. The effect would be similar if we consider the enhancement occurring due to the random steps on the surface. This is not the case when we see the SHG pattern for Pin/Pout polarization combination shown in Fig. 4, and so this candidate is eliminated.

B. Electronic resonance of Au/TiO₂ interface step

An electronic resonance may occur at the step region of the Au/TiO₂ interface. J. R. Power *et al.* observed an enhancement of SHG signal from a stepped Si (001) surface due to the strong electronic resonance.²⁹ T. F. Heinz *et al.* observed SHG and SFG spectra due to the electronic resonance from the CaF₂/Si (111) interface. This electronic resonance occurred due to the interband electronic transition at the interface by the excitation by one photon.³⁰ In our study we observed the enhanced SHG signal (shown in Fig. 6) correlated with the existence of the Au/TiO₂ (320) interface steps. Hence this is a credible candidate the interface step electronic state being the origin of our signal.

C. Surface plasmon effect on SHG enhancement

The collective oscillations of the free electrons may occur in metal surface such as silver, gold or copper induced by the interacting electromagnetic field and they are known as surface plasmons.³¹ In the case of a thin gold film deposited on pre-patterned TiO₂ substrate, local field enhancement may result from the surface plasmon resonance (SPR). Then the SHG intensity is non-linearly dependent on the local field enhancement factors.³² In order to check the influence of SPR on the enhancement of the anisotropic SHG signal, we measured the linear reflectivity of our sample at $\varphi = 0^\circ$ and 180° as shown in Fig. 7. In Fig. 7 the decrease of reflectivity for the p-polarization above 600 nm might be due to the contribution of SPR. Nevertheless, the reflectance at $\varphi = 0^\circ$ and 180° were found to be approximately the same as each other for both P- and S- polarized excitation light. Thus the incident field of frequency ω makes approximately the same local field in the sample at $\varphi = 0^\circ$ and 180° . So the different enhancement of SHG signal between $\varphi = 0^\circ$ and 180° should not occur owing to SPR.

D. Fresnel factor effect on SHG enhancement

The intensity of the surface second harmonic signal per laser pulse $I(2\omega, l, \varphi)$ is given by the following equation³³

$$I(2\omega, l, \varphi) \propto |L(2\omega, l, \varphi) \chi^{(2)}(l, \varphi) L(\omega, l, \varphi)|^2 I^2(\omega) \quad (2)$$

Here, $L(\omega, l, \varphi)$ and $L(2\omega, l, \varphi)$ are the Fresnel factors at frequencies of ω and 2ω respectively, and $I(\omega)$ is the intensity of the incident laser pulses. The parameter l indicates the polarization of the light

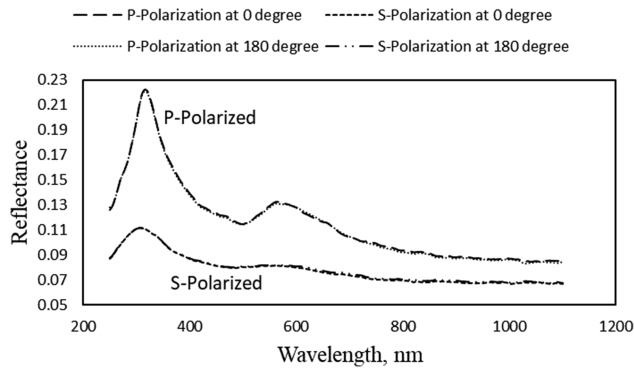


FIG. 7. Linear reflectivity curve of Au/TiO₂ (320) sample for both P- and S- polarized light at $\varphi = 0^\circ$ and 180° as a function of wavelength.

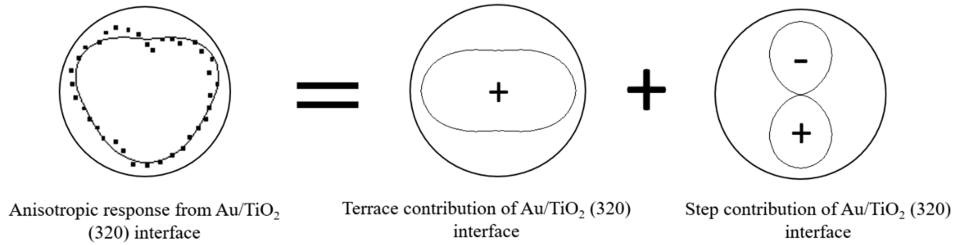


FIG. 8. The anisotropic response for Pin/Pout polarization combination from the Au/TiO₂ (320) interface at excitation light with photon energy 2.33 eV separated into the step and terrace contributions.

wave and is either s or p. The parameter φ indicates the sample rotation angle. The Fresnel factor $L(\omega, l, \varphi)$ indicates how much light field at frequency ω is generated inside the nonlinear medium by the incident light by the linear optical process.²⁶ From our linear measurement, we confirmed that the linear reflectivity spectra are the same between the rotation angles $\varphi = 0^\circ$ and 180° as shown in Fig. 7. The fact that the reflectivity spectra are exactly the same means that the Fresnel factors are the same between the rotation angles $\varphi = 0^\circ$ and 180° . Hence the enhancement of the SHG signal should only be due to the φ -dependence of the $\chi^{(2)}(l, \varphi)$ term in Eq. (2). So, the influence of the Fresnel factors on the enhancement of SHG signal can be eliminated.

From the above discussion of four candidates, it seems that only candidate (b) is feasibly responsible for the enhancement of the SHG. In this case, the electronic resonance at the Au/TiO₂ (320) interface step may have caused the enhancement of the SHG signal.

Although it is difficult to conclude the exact origin of the enhancement of the SHG intensity considering the step contributions of Au/TiO₂ (320) compared to the bare TiO₂ (320) sample, we have succeeded in decomposing theoretically the nonlinear susceptibility elements of anisotropic and isotropic symmetry from the experimental data. There are two groups of the nonlinear susceptibility elements corresponding to step and terrace contribution to the SHG response. These two components give positive interference at $\varphi = 180^\circ$ and negative interference at $\varphi = 0^\circ$ as we show it in Fig. 8. As the next step it is important to perform the photon energy dependence of the SHG response. At that step, the separation of the SHG response as in Fig. 6 is necessary to discuss the terrace and step contribution.

V. CONCLUSION

We obtained SHG intensity patterns from the Au/TiO₂ (320) and bare TiO₂ (320) samples as a function of the polarization combinations and azimuthal angle. The isotropic response was observed from both samples with the excitation photon energy of 1.17 eV. On the other hand, at photon energy 2.33 eV, the anisotropic SHG signal was measured from both the Au/TiO₂ (320) and bare TiO₂ (320)

samples. Our analysis suggests that, after eliminating other candidate mechanisms, an electronic resonance at the Au/TiO₂ (320) interface step is the major contributor to the relevant $\chi_{ijk}^{(2)}$ elements.

ACKNOWLEDGMENTS

This work was supported by JSPS KAKENHI Grant Number JP15K05126.

- ¹ Z. Duan and G. Henkelman, *ACS Catal.* **5**, 1589–1595 (2015).
- ² Q. Yao, C. Wang, H. Wang, H. Yan, and J. Lu, *J. Phys. Chem. C* **120**, 9174–9183 (2016).
- ³ M. Valden, S. Pak, X. Lai, and D. W. Goodman, *Catal. Lett.* **56**, 7–10 (1998).
- ⁴ M. Haruta, *Catalysis Today* **36**, 153–166 (1997).
- ⁵ M. Haruta, S. Tsubota, T. Kobayashi, H. Kageyama, M. J. Ganet, and B. Delmon, *J. Catal.* **144**, 175 (1993).
- ⁶ S. Tsubota, T. Nakamura, K. Tanaka, and M. Haruta, *Catal. Lett.* **56**, 131 (1998).
- ⁷ T. Minato, H. Kato, and M. Kawai, *Journal of Surface Science Society of Japan* **27**, 319–325 (2006).
- ⁸ H. Takahashi, R. Watanabe, and G. Mizutani, *e-J. Surf. Sci. Nanotech.* **8**, 84–88 (2010).
- ⁹ X. Lai, T. P. St. Clair, M. Valden, and D. W. Goodman, *Surface Science* **59**, 25–52 (1998).
- ¹⁰ T. Tanaka, A. Sumiya, H. Sawada, Y. Kondo, and K. Takayanagi, *Surface Science* **619**, 39–43 (2014).
- ¹¹ A. Aiboushev, A. Astafiev, O. M. Sarkisov, and V. A. Nadochenko, *Journal of Physics* **291**, 012040 (2011).
- ¹² Z. K. Zhou, M. Li, X. R. Su, Y. Y. Zhai, H. Song, J. B. Han, and Z. H. Hao, *Phys. Stat. Sol. (A)* **205**, 345–349 (2008).
- ¹³ C. Zhang, Y. Liu, G. You, B. Li, J. Shi, and S. Qian, *Physica B* **357**, 334–339 (2005).
- ¹⁴ M. Kyoung and M. Lee, *Bull. Korean Chem. Soc.* **21**, 1 (2000).
- ¹⁵ X. Quelin, J. Sakars, A. Bourdon, and P. Gadenne, *Physica B* **279**, 102–104 (2000).
- ¹⁶ L. Marrucci, D. Paparo, G. Cerrone, C. de Lisio, E. Santamato, S. Solimeno, S. Ardizzone, and P. Quagliotto, *Optics and Lasers in Engineering* **37**, 601–610 (2002).
- ¹⁷ J. J. H. Gielis, P. M. Gevers, I. M. P. Aarts, M. C. M. Van de Sanden, and W. M. M. Kessels, *J. Vac. Technol. A* **26**(6) (2008).
- ¹⁸ S. Cattaneo, E. Vuorimaa, H. Lemmetyinen, and M. Kauranen, *J. Chem. Phys.* **120**(19) (2004).
- ¹⁹ E. Kobayashi, T. Wagasugi, G. Mizutani, and S. Ushioda, *Surface Science* **402-404**, 537–541 (1998).
- ²⁰ M. Omote, H. Kitaoka, E. Kobayashi, O. Suzuki, K. Aratake, H. Sano, G. Mizutani, W. Wolf, and R. Podloucky, *Journal of Physics: Condensed Matter*. **17**(8), S175–S200 (2005).
- ²¹ H. Takahashi, R. Watanabe, Y. Miyauchi, and G. Mizutani, *J. Chem. Phys.* **134**, 154704 (2011).
- ²² M. W. Ribarsky, *Hand Book of Optical Constants of Solids* ed E.D. Palik (San Diego, CA: Academic) p.795 (1985).
- ²³ N. K. Quang, Y. Miyauchi, G. Mizutani, M. D. Charlton, R. Chen, S. Boden, and H. Rutt, *Jpn. J. Appl. Phys.* **53**, 02BC11 (2014).
- ²⁴ P. F. Brevet, *Surface Second Harmonic Generation*, Press polytechniques et universitaires romandes, pp. 69–71, 133–134 (1996).
- ²⁵ E. Kobayashi, G. Mizutani, and S. Ushioda, *Jpn. J. Appl. Phys.* **36**, 7250 (1997).
- ²⁶ A. G. Lambert, P. B. Davies, and D. J. Neivandt, *Appl. Spectrosc. Rev.* **40**, 103 (2005).
- ²⁷ D. L. Mills, *Nonlinear Optics Basic Concepts*, 2nd edition (Springer, 1998), pp. 173–174.
- ²⁸ C. K. Chen, A. R. B. de Castro, and Y. R. Shen, *Phys. Rev. Lett.* **46**, 145 (1981).
- ²⁹ J. R. Power, J. D. O’Mahony, S. Chandola, and J. F. McGilp, *Phys. Rev. Lett.* **75**, 1138–1141 (1995).
- ³⁰ T. F. Heinz, F. J. Himpsel, and E. Palange, *Phys. Rev. Lett.* **63**(6) (1989).
- ³¹ A. Lesuffleur, P. Gogol, P. Beauvillain, B. Guizal, D. Van Labeke, and P. Georges, *J. Appl. Phys.* **104**, 124310 (2008).
- ³² C. Hubert, L. Billot, P.-M. Adam, R. Bachelot, P. Royer, J. Grand, D. Gindre, K. D. Dorkenoo, and A. Fort, *Appl. Phys. Lett.* **90**, 181105 (2007).
- ³³ P. J. Campagnola, M. Wei, A. Lewis, and L. M. Loew, *Biophysical Journal* **77**, 3341–3349 (1999).